ANNALES
UNIVERSITATIS MARIAE CURIE-SKLODOWSKA
LUBLIN—POLONIA
VOL. XXXIX/XL, 8 SECTIO AA 1984/1985

Zakład Chemii Analitycznej i Analizy Instrumentalnej
Instytut Chemii UMCS

Ewa CUKROWSKA, Ignacy CUKROWSKI,
Kazimierz SYKUT

The Influence of Carbon and Graphite Substrates on Electrochemical Properties of Epoxy-resin-impregnated Electrodes in Voltammetric Measurements. Part III. The Characteristics of Hg-film Electrodes in an Aspect of ASV Measurements

Wpływ rodzaju tworzywa węglowego i grafitowego na elektrochemiczne właściwości impregnowanych żywicą epoksydową elektrod do miarów woltamperometrycznych. Część III. Charakterystyka błonkowych elektrod rtęciowych w aspekcie pomiarów metodą odwróconej woltamperometrii

Влияние вида угольного и графитного материала на электрохимические свойства импрегнированных эпоксидной смолой электродов для вольтамперметрических измерений. Часть III. Характеристика пленочных ртутных электродов в аспекте измерений методом обратной. вольтамперметрии

INTRODUCTION

Two previous part [1,2] described technology of defined composition electrode rods and presented investigations carried out in the positive range of potentials on eletrochemical applicability of epoxy-resin-impregnated electrodes [3,4] made of these rods.

It has been known that mercury film in the form of single very small mercury droplets is obtained on the graphite and carbon substrates [5-7]. Štulikova [7], studied on GC rotating electrode the influence of mercury film deposition potential on coverage homogeneity as well as on reversibility of mercury reduction and oxidation processes. Morcos [8, 9] studied the electrochemical reduction of mercuorous ion on both cleavage and

edge orientations of high pressure stress-annealed pyrolitic graphite. Electrodeposition and stripping of Hg at graphite cloth electrodes have also been a subject of investigations [10]. There has been carried out spectroelectrochemical observation of mercury phase growth on glassy carbon [11]. M a t s o n at wal. [5] on the basis of microscopic observations have stated that on the wax-impregnated graphite electrodes 1/10 of mercury is obtained in the droplet form of about 0,01 mm diameter, the rest is apparently in the form of much smaller droplets beyond the resolving power of the microscope used.

However, influence of material kind and electrode rod technology (saturation, burning off, graphitization) on the structure of mercury deposit and electrochemical properties of mercury film covered epoxy-resin-impregnated electrodes has not been discussed in literature so far. It is a subject of this paper.

EXPERIMENTAL

Reagents and solutions

The solutions were prepared with reagent grade or Suprapur chemicals and twice-distilled water. Standard solutions with the known Zn, Cd, Pb and Cu contents were prepared by diluting 0,1 M solutions with redistilled water and stored in polyethylene bottles rinsed with acid. Redistilled water was used throughout. The solutions were strirred during the plating period by a metered high-purity nitrogen stream, which was also used to deoxygenate the solutions. All the experiments were performed at ambient room temperature.

Instruments and electrodes

All voltammetric curves were recorded using a threeelectrode arrangement with an instrumentation consisting of multiple voltammetric analyser with programming of measurements, which was built in our laboratory- equipped with an N306 X-Y recorder (USSR). As a reference electrode the saturated calomel electrode was used.

RW Ia

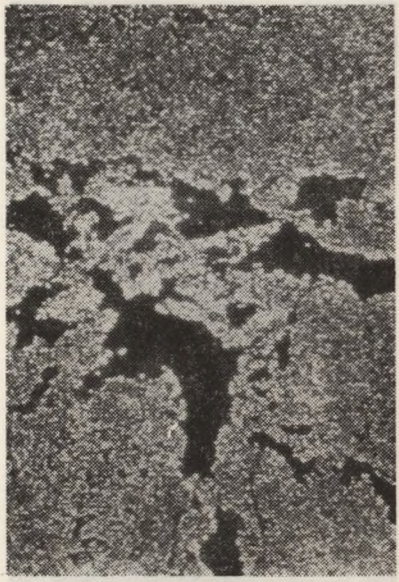

RW Ib

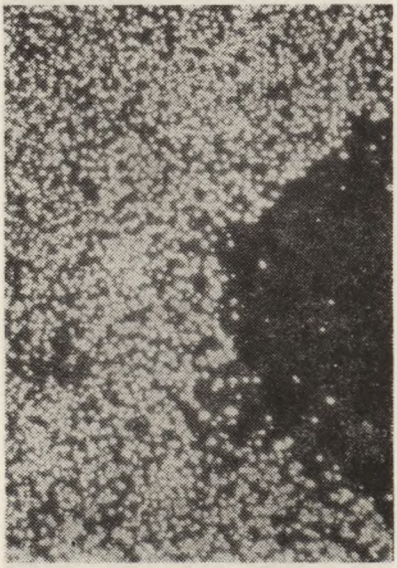

RW IIa

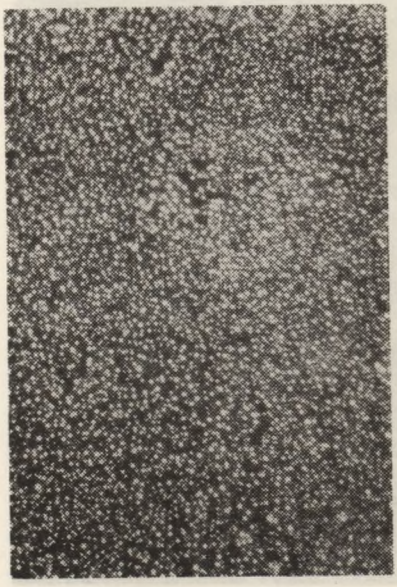

RW IIb

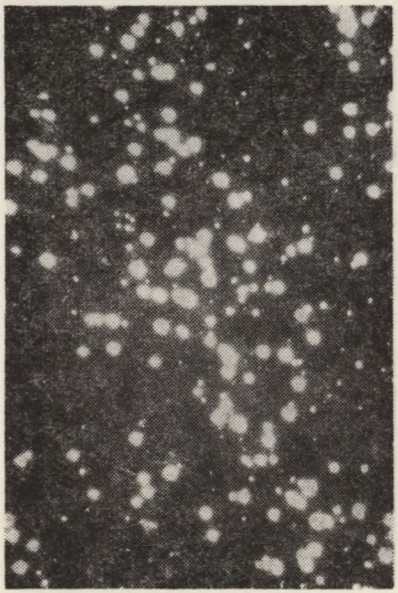

ELS 1a

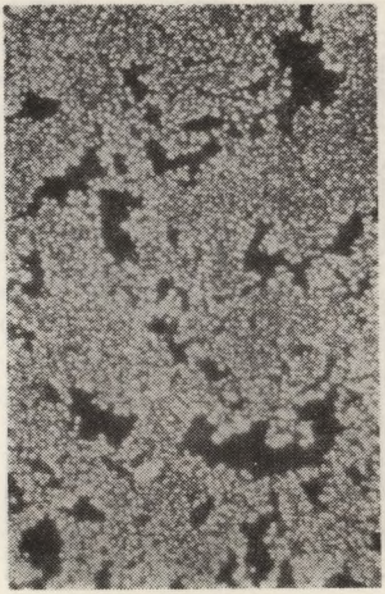

ELS 1b

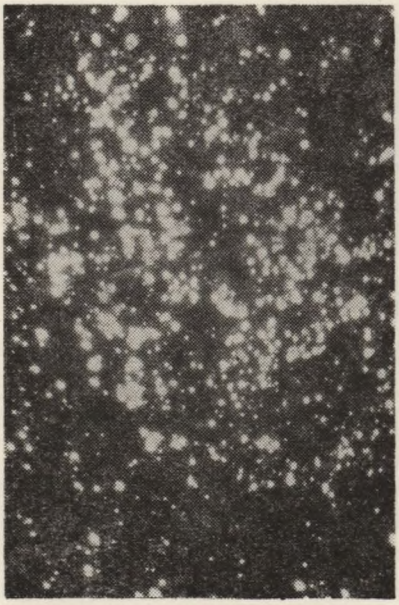

ELS 2a

ELS 2b

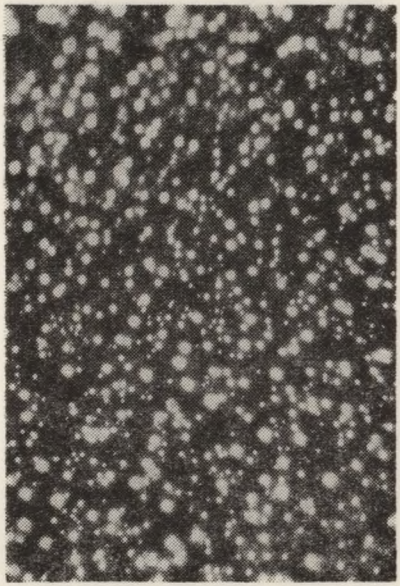

GC a

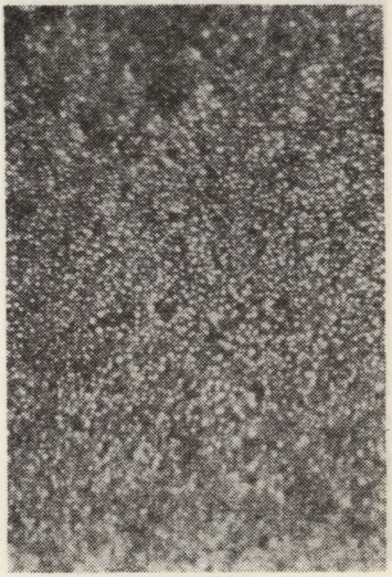

GC b

ROM 1a

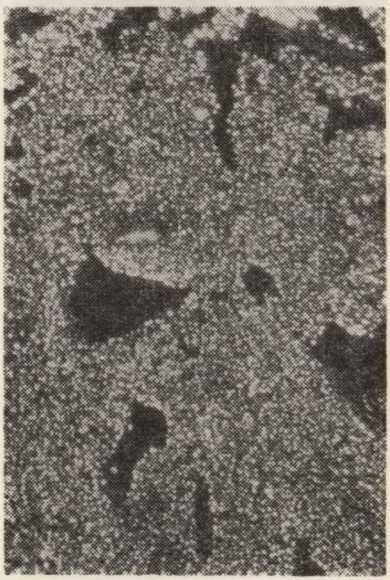

ROM 1b

ROM 2a

ROM 2b

ROM 3a

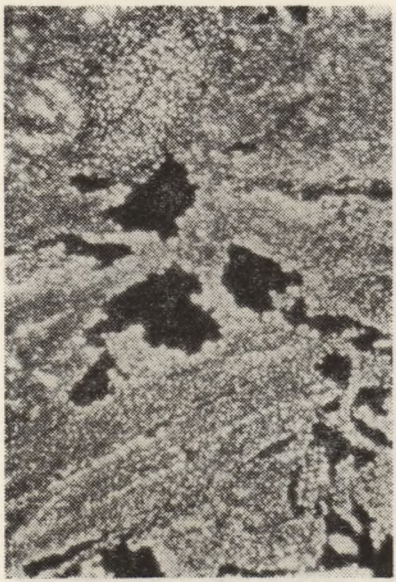

ROM 3b

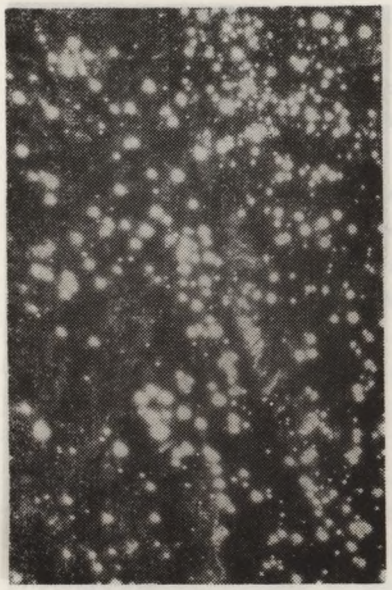

CON 2 | a

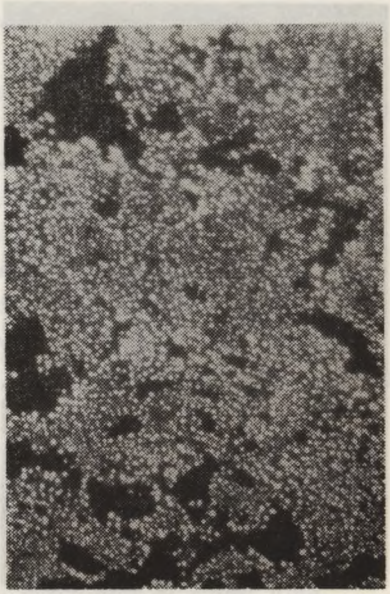

CON 2 | b

Fig. 7. The microscopic photographs (dark field method) of mercury films deposited on electrode electroactive surface at deposition potential: (a) — −0.7 V, (b) — −1.4 V. Solution: 0.1 M $HClO_4$, $1 \cdot 10^{-4}$ M Hg^{2+}. Deposition time 3 min. Magnification 800×

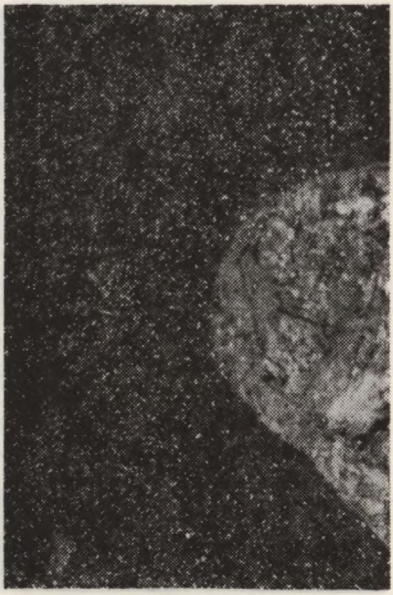

RW IIa

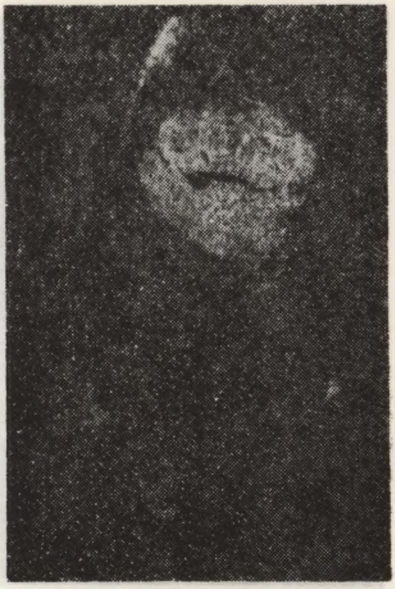

RW IIb

ROM 2a

CON 2b

Fig. 8. The microscopic photographs (bright field method) of mercury films deposited on electrode electroactive surface at deposition potential: (a) — −0.7 V, (b) — −1.4 V. All other data are given in Fig. 7

Electrochemical deposition of mercury film

Mercury films were deposited on impregnated electrodes (IE) and GC from the solution 1.10^{-4} M Mg^{2+} in 0,1M $HClO_4$. For each electrode mercury deposition took place from a new portion of solution. The solution in the vessel was deoxidized for 10 min. each time. Mercury was deposited at the potentials of -0.7 V and -1.4V in the second series (intensive evolution of hydrogen). Deposition time of mercury films was always 3 min. The solutions were stirred during the plating period by nitrogen using the method of striking gas [12]. Gas outflow speed from the capillary was $800 cm \cdot s^{-1}$ which corresponds to gas outflow efficiency of $150 ml \cdot min^{-1}$. The electrode with the deposited mercury film was taken out of the solution, rinsed with redistilled water and allowed to dry which took about 1 min. The electrode prepared in this way was placed in a holder making perpendicular position to optical axis of the photographed surface possible. Surface photographs were made at magnification of 800x and at white light. The surface of each electrode was photographed twice using the method of bright and dark field [13]. Then to check reproducebility of experimental conditions a series of photographs was made for a few chosen electrodes. After that mercury films on all IE and GC as well as their photographs were obtained in the way described above (at the deposition potentials of -0.7V and -1.4V). A part of the obtained material (from about 60 photographs) was chosen as an illustration in discussion.

ASV on mercury film electrodes

ASV measurements were carried out in 0.01M and 0.05M H_2SO_4 solutions including Zn, Cd, Pb and Cu ions. The concentration of each depolarizer was $1 \cdot 10^{-7}$ M. Mercury film was deposited in situ whereby mercury ion concentration was $5 \cdot 10^{-5}$ M. 10 ml of the studied sample was poured into a measuring vessel and deoxidized for 10 min. by nitrogen stream. With continuous stirring, preliminary deposition electrolysis was carried out for 2 min. at the potential of -1.4V. Then the deposited metals were dissolved from the electrode surface at the potential of +0.2V without mercury film dissolution. When the potential was changed to -1.4V metals were deposited during 3 min.

Then gas was passed over the solution. After 30s. ASV curves were recorded with the scan rate of potential 5V.min^{-1}.

From the registered ASV curves potential and current values of anodic metal dissolution peaks were determined. Current values estimated from ASV curves were converted to a surface electrochemical unit (1 cm^2) of each electrode (electrochemical surface of each electrode was estimated in ferri- and ferrocyanide solutions using chronoamperometric method). The estimated E_p and converted i_p are given in Figs. 1,2.

Lead i_p^a and E_p^a dependence on scan rate of potential

Investigations were carried out on ELS 2 electrode in 0.1M $HClO_4$ solution which included $2.5 \cdot 10^{-5}$M Hg^{2+} and 3.10^{-7}M Pb^{2+}. In all measurements deposition time was 10 min. and V_e was -1.0V. After each measurement mercury film was dissolved and mercury oxidation peak registered at the same time. From the determined charge of mercury film oxidation (the average 615 μC) the average thickness of mercury film was estimated to be 37,5Å (assuming for simplicity that mercury forms and uniform layer on the electrode surface). The same solution was used to estimate the halfwave potential of Pb from the lead reduction voltammetric curve on a HMDE ($E_{1/2}$ = -389 mV). The obtained data are presented in Tab. 1 and Figs. 3, 4.

Lead i_p^a and E_p^a dependence on time of deposition electrolysis and mercury film thickness

Investigations were carried out on ELS 2 electrode in the solution of 0.1M $HClO_4$ which included $2 \cdot 10^{-4}$M Hg^{2+} and $3 \cdot 10^{-7}$M Pb^{2+}. The deposition potential was -0.9V and voltage scan rate 0.01V$\cdot$s^{-1}. Mercury film thickness was changed using different time of electrolysis. Both Pb and Hg dissolution peaks were recorded. Charges over peaks were estimated from mass of the cut off peaks. The obtained data are presented in Tab. 2 and in Figs. 5, 6.

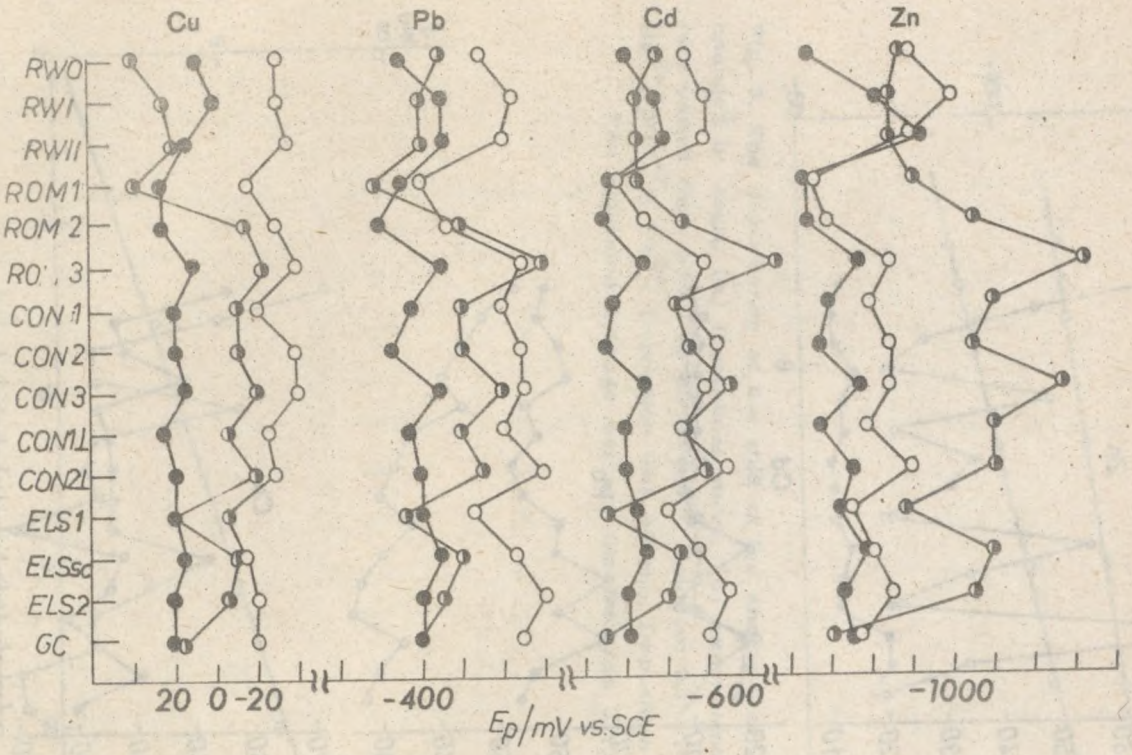

Fig. 1. The potentials of anodic metal dissolution peaks obtained at tested IE and GC electrodes in solutions: ○ - 0,05M H_2SO_4, t_e = 3 min., ◒ - 0,01M H_2SO_4, t_e = 2 min., ● - 0,01M H_2SO_4, t_e = 3 min. Deposition potential - 1,4V. Scan rate 0,083Vs^{-1}. The concentration of each depolarizer $1 \cdot 10^{-7}$M., $c_{Hg^{2+}} = 5 \cdot 10^{-5}$M

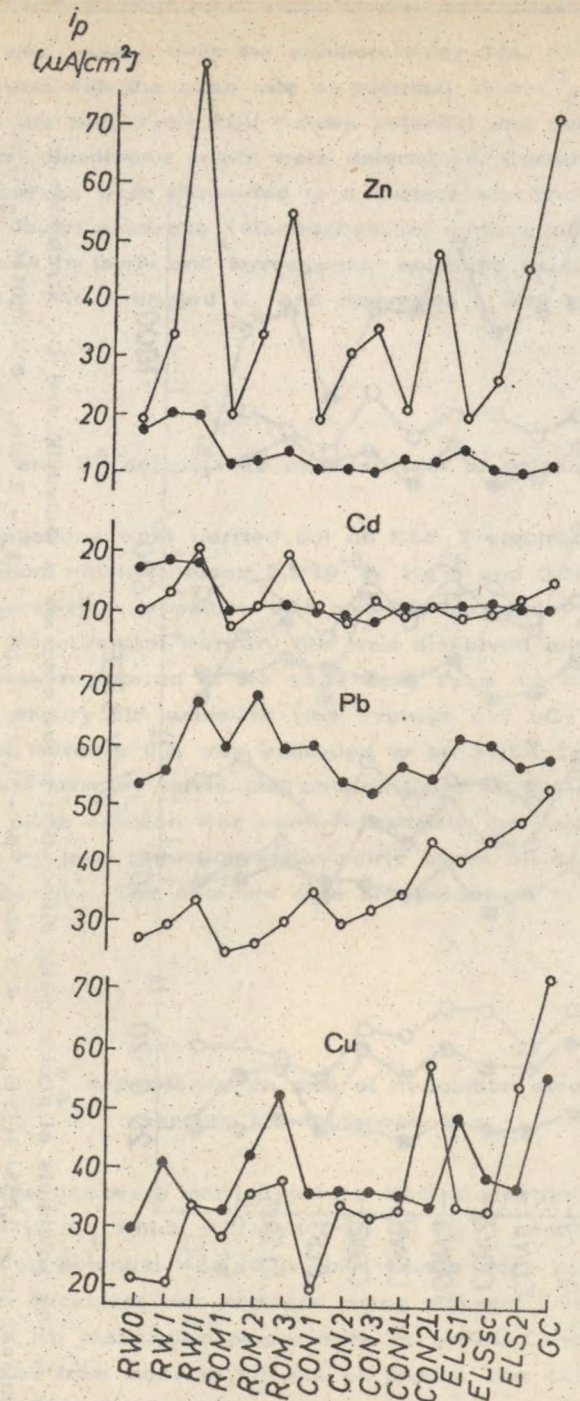

Fig. 2. The converted current values from ASV curves to a surface electrochemical unit ($1cm^2$) of each tested electrode. All data are given in Fig. 1

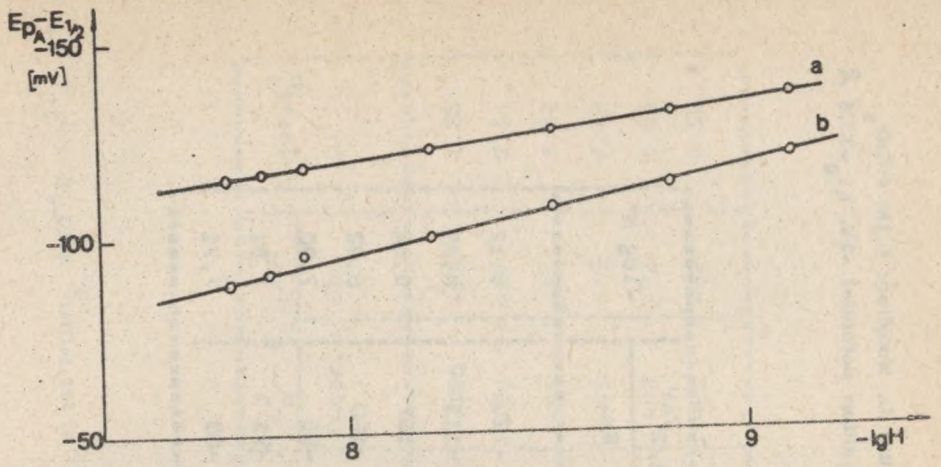

Fig. 3. The dependence of the shift of the anodic lead peak on the changes in -logH. (a) theoretical curve, (b) experimental curve. Scan rate varied from $1 \cdot 10^{-3}$ to $25 \cdot 10^{-3} Vs^{-1}$. Solution: 0.1M $HClO_4$, $2.5 \cdot 10^{-5}$M Hg^{2+}, $3 \cdot 10^{-7}$M Pb^{2+}. Deposition time 10 min. Deposition potential - 1V. The estimated average mercury film thicknes 37.5Å

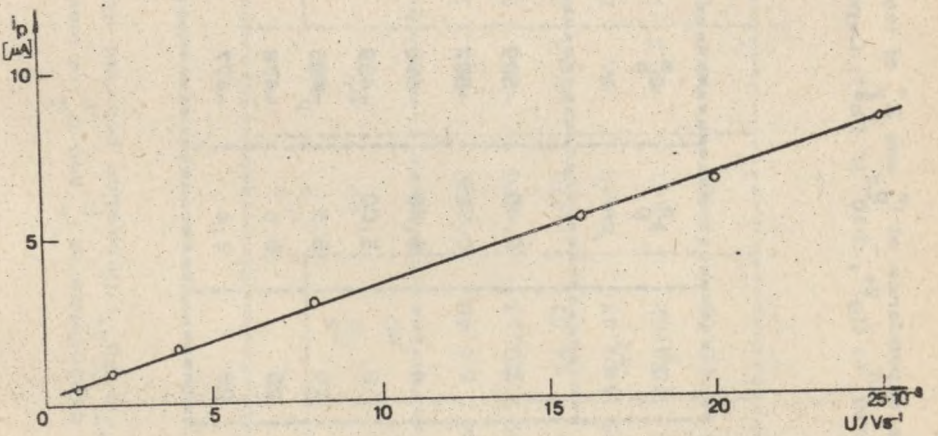

Fig. 4. The experimental dependence of the anodic lead peak height on scan rate of potential. All data given in Fig. 3

Table I. The dependence of i_p^a and E_p^a of lead on scan rate of potential U. Solution: 0.1M $HClO_4$, $2.5 \cdot 10^{-5}$M Hg^{2+}, $3 \cdot 10^{-7}$M Pb^{2+}. Deposition time 10 min. Deposition potential -1V. l_{Hg}=37,5 Å

$10^3 U$ Vs^{-1}	i_p^a μA	E_p^a mV	$b_{1/2}$ mV	$E_p^a - E_{1/2}$/mV		-log H
				Theor.	Ex.	
1	0,46	-509	38	-135	-120	9,12
2	0,885	-502	40,8	-131	-113	8,82
4	1,69	-496	38,4	-127	- 107	8,52
8	3,00	-489	43,6	-122	-100	8,22
16	5,5	-485	46,0	-118	-96	7,90
20	6,6	-478	43,2	-116	-91	7,81
25	8,4	-477	48,0	-115	-88	7,71

Table II. The dependence of i_p^a and E_p^a of lead on t_e and l_{Hg}. Solution: 0.1M $HClO_4$, $2 \cdot 10^{-4}$M Hg^{2+}, $3 \cdot 10^{-7}$M Pb^{2+}. Deposition potential -0.9V. Scan rate 0.01Vs^{-1}

t_e min	Pb		E_p^a	$b_{1/2}$	Hg		$10^7 H$	$E_p^a - E_{1/2}$/mV		Theor. i_p^a
	i_p^a μA	Q_p^a μC	mV	mV	Q_p^a mC	l Å		Theor.	Ex.	μA
2	1,02	5,46	-482	45	1,90	116	0,725	-106	-93	1,26
4	1,95	10,13	-476	45	3,34	204	2,25	-99	-87	2,34
6	2,9	14,57	-470	45,6	4,62	282	4,29	-95	-81	3,37
8	3,75	19,43	-465	42	6,31	385	8,01	-91	-76	4,49
10	4,7	24,62	-461	44,4	7,50	458	11,13	-89	-72	5,69
12	5,5	28,51	-458	44	8,87	541	15,8	-86	-69	6,59

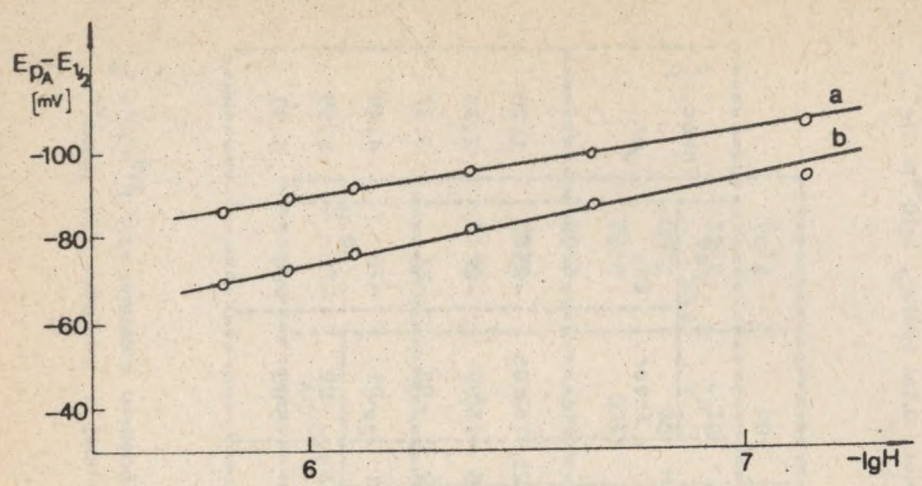

Fig. 5. The dependence of the shift of the anodic lead peak on the changes in -logH. (a) theoretical curve, (b) experimental curve. Deposition time varied from 2 to 12 min. The estimated mercury film thickness varied from 116 to 541 Å. Solution: 0.1M $HClO_4$, $2 \cdot 10^{-4}$M Hg^{2+}, $3 \cdot 10^{-7}$M Pb^{2+}. Scan rate 0.01Vs^{-1}. Deposition potential -0.9V

DISCUSSION

From the analysis of the photographs of mercury film covered IE and GC it can be stated that mercury coverage i.e. drop size, coverage homogeneity and distribution of droplets depends on such factors as: kind of the rod (composition), technology (burning off, graphitization), electrochemical measurement conditions (value of deposition potential) and also on way of solution stirring or on preparing working electrode active surface for measurements. In spite of complexity of the problem, the experiments carried out provide conclusions of more general type. It was stated that not only in the case of glassy carbon electrodes [7] but on all kinds of studied electrodes (part 1) with increase of deposition potential negative values, finer and denser mercury coverage is obtained Fig. 7. Moreover, it can be seen that at the same V_e values

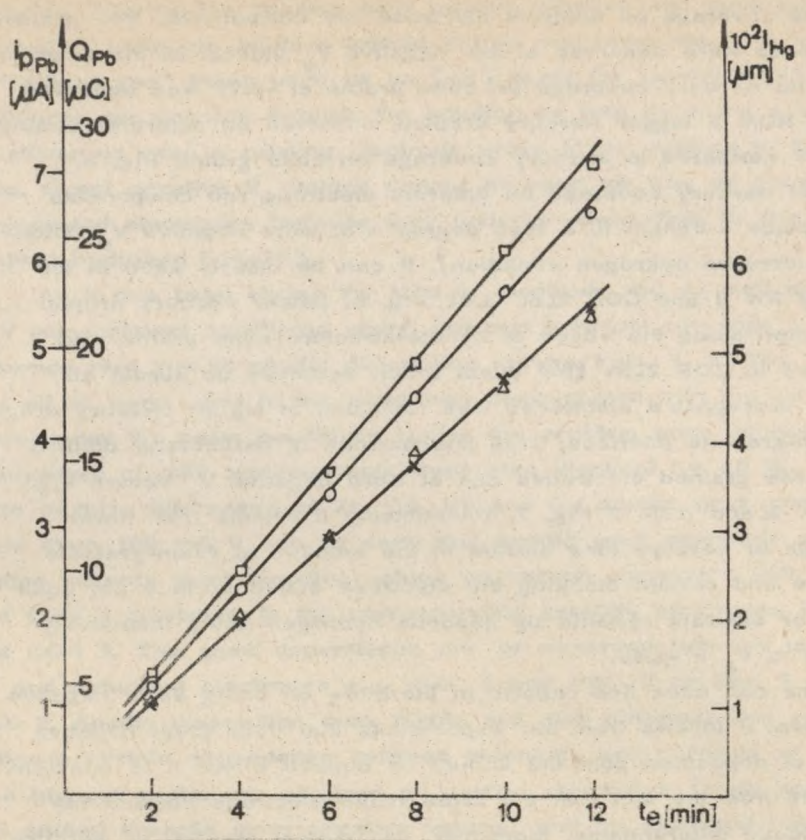

Fig. 6. The dependence of theoretical and experimental anodic lead peak height, mercury film thickness and charge of lead oxidation on deposition time. (o) calculated peak height, (x) experimental peak height, ( ) charge of lead oxidation, ( ) mercury film thickness.
Solution and other data are given in Fig. 5

mercury droplets on carbon substrates (RW II, GC, ROM3) are considerable bigger compared to graphite ones.

Saturation of electrode rods proved to exert additional influence on mercury coverage. Saturated graphite electrodes are characterized by finer mercury coverage than corresponding unsaturated graphite ones at the same V_e values Fig. 7. (ROM 1 and ROM 2 or ELS 1 and ELS 2 at V_e = -0.7V and -1.4V). The photographs clearly show

different coverage on different electrode rod components. The greatest differences were observed at low negative V_e values. In the case of RW II no mercury coverage on coke grains at -0.7V was observed and of ROM 2 bigger mercury droplets occurred on saturant remains at -0.7V compared to mercury coverage on coke grains Fig. 8. Different mercury coverage on different electrode rod components takes place - though to a less degree - at more negative V_e potentials (intensive hydrogen evolution). It can be clearly seen in the case of RW II and CON 2L at -1.4V Fig. 8. Linear mercury droplet distribution along the edges of needle-structure coke grains was observed in CON 2L.A fine effect which occurred on almost all studied impregnated electrodes was formation of bigger mercury droplets in resin-graphite interface. This phenomenon is particularly distinct for coarse grained electrodes and at more negative V_e values e.g. on CON 2L and ROM 2 Fig. 7. Undoubtedly it results from lower decrease of mercury ions amount in the solution at resin-graphite interface and certain blocking the electrode active surface i.e. coke grains or saturant remains by gaseous hydrogen being intensively evolved at V_e = -1.4V.

One can often find reports in literature on using small negative V_e values. It follows from our experiments that very great negative values of deposition potential should be applied where it is possible. It results from the fact that the impregnated electrode surface is energetically differentiated. Moreover, mechanical removal of mercury film is a normal analytical procedure. It causes different behaviour of a newly polished electrode in comparison with the electrode where mercury was removed in a mechanical way. Hence, there are some suggestions that also glassy carbon electrodes should be polished after each measurement. In our opinion in some cases it is not necessary. It is sufficient to polarize the electrode in the area of hydrogen evolution potential which is confirmed by e.g. photographs of ELS 1 electrode surface with mercury deposited at -0.7V and -1.4V Fot. 10. Great negative V_e values not only decreases mercury droplet diameter but above all causes electrochemical purification of IE active surface. It causes electrochemical activity restoration of the whole electrode surface, therefore approximation of the determined electrochemically active surface to the calculated geometrical electrode surface. It should be kept in mind that not every method of solution stirring allows V_e to be used in the potential area of intensive hydrogen

evolution. Stirring the solution must ensure effective and continuous removal of hydrogen bubbles formed during measurements. The method of "Striking gas" being used by us [12] meets the condition but traditional gas passing through the solution as well as using a magnetic stirrer or even a rotating electrode prove to be useless in this case. Great negative V_e values cannot be used for wax or paraffin impregnated electrodes because they undergo destruction by the evolved hydrogen [14-16].

As it has been shown the kind of electrode rod as well as ASV measurement conditions giving different mercury coverage influence also run of anodic dissolution curves Figs. 1, 2. The fact that all IE were made in the same way, impregnated with the same resin under the same conditions makes the problem more interesting. Parameters of ASV measurements were also identical for all IE. In spite of this, differences of Zn, Cd, Pb and Cu anodic peak potentials yield even 100 mV. It can be seen that anodic peak potentials are shifted towards more negative values on carbon electrodes RON 3 and CON 3 compared to the corresponding graphite electrodes RON 1 and CON 1. The same dependence can be observed between unsaturated and saturated electrodes e.g. RON 1 and RON 2 or ELS 1 and ELS 2. Anodic dissolution peak hights are also different. One can notice a certain dependence between potentials and currents of peaks. The highest peaks are obtained on carbon electrodes (peak potentials are shifted towards more negative values) and on saturated electrodes compared to the corresponding unsaturated ones. It should be stressed that all measurements (Figs. 1, 2) were carried out at V_e --1.4V (intensive hydrogen evolution), therefore under the conditions giving possibly the most homogeneous and complete mercury coverage on all studied electrodes. Significant defferences of peak potentials and currents may point to an action between the electrode substrate and mercury film with metals deposited in it or to different electrochemical activity of different mercury coverage obtained on the tested electrodes. The results presented in Fig. 9 can be treated as confirmation of the above suggestion where on one chosen electrode RON 1 mercury and lead were deposited either at the same or different V_e. On the basis of the presented results different interpretations of Cu dissolution double peak by various authors [17, 18] becomes quite clear. In our opinion both interpretations do not exlude each other because at very heterogeneous mercury coverage of graphite

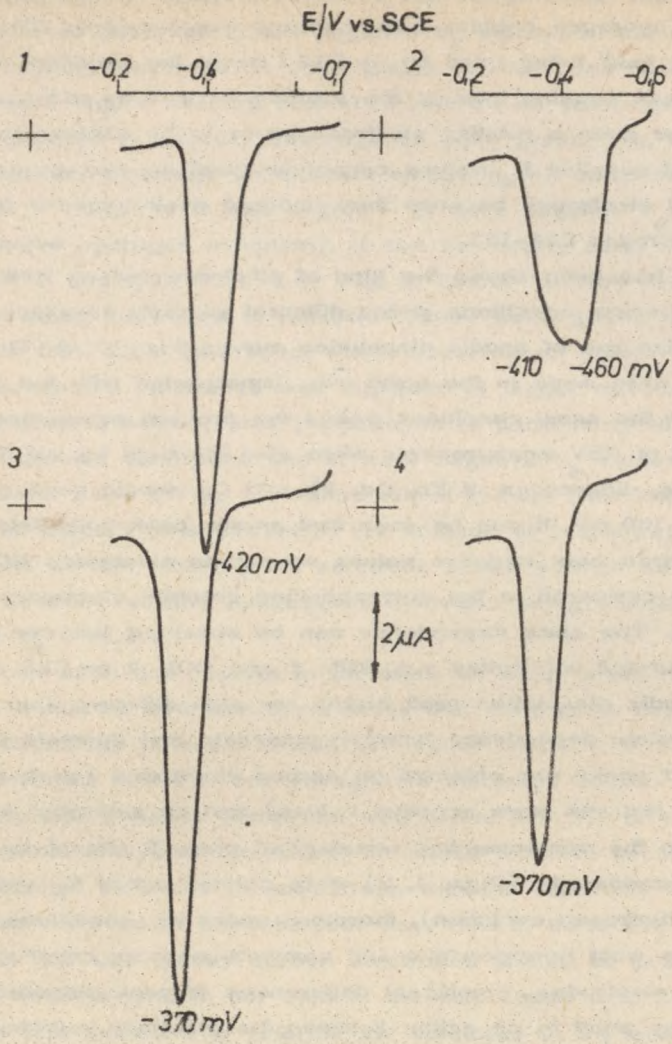

Fig. 9. The dependence of anodic lead peak height on mercury film deposition potential. ROM 1 electrode. Solution: 0.05M H_2SO_4, $5 \cdot 10^{-7}$M Hg^{2+}, $1 \cdot 10^{-7}$M Pb^{2+}. Scan rate $0.083 Vs^{-1}$. Deposition time 3 min. 1. $V_{e_{Hg}} = -0.7$ V $V_{e_{Pb}} = -0.7V$; 2. $V_{e_{Hg}} = -0.7V$ and next -1.4 V $V_{e_{Pb}} = -1.4$ V; 3. $V_{e_{Hg}} = -1.4V$ and next -0.7V $V_{e_{Pb}} = -0.7V$; 4. $V_{e_{Hg}} = -1.4$ V $V_{e_{Pb}} = -1.4V$

substrate (significant differences in diameter of mercury droplets [17]) supersaturated Cu amalgam can be formed which leads to double oxidation peak also observed in the case of silver based mercury film electrode [19].

Considering the obtained results in the aspect of the most developed and verified de Vries and Van Dalen's theory [20], it can be stated that this theory is only an approximation of real conditions when graphite or carbon electrode is employed. It results from the fact that it describes electrochemical dependences for film electrodes where homogeneous mercury film actually exists. The non-dimensional parameter $H = l^2 a/D_r$ (where $a=nFU/RT$) introduced by them, allowing to obtain theoretical curves under the defined experimental conditions, includes l - mercury film thickness (cm) but not a constant describing actual mercury coverage or an action between mercury and substrate. Moreover, the formulae of cathodic and anodic peaks assume that electrode surface A corresponds to geometrical surface of mercury film substrate which is not true.

Dependence of lead oxidation peak potential on voltage scan rate presented in Fig. 3 has a linear run. It is in agreement with de Vries and Van Dalen's theory but lead oxidation peaks are of about 20mV shifted towards positive values. This shift increases with U increase to a greater degree than it was predicted in the theory. In spite if these divergences $i_p = f(U)$ has a linear run according to the theory which is decisive for an analyst - Fig. 4. Similarly the dependence $(E_p^a - E_{1/2}) = f(U)$ - Fig. 5 has a linear shape and runs below the curve predicted by the theory. In this case also with the increase of the parameter H the distance between the theoretical curve and that obtained in the experiment increases insignificantly. It probably results in this case from better mercury film coverage of the substrate - Fig. 6.

Great care should be taken in the studies of agreement between experimental data obtained bn film electrodes made of graphite or carbon and predicted theoretical values in the case of homogeneous film occurence. When there are maintained basic dependences i.e. linear dependence between peak current and deposition electrolysis time, potential scan rate and metal concentration in the solution or dependence between shift direction of dissolution potential peak and potential scan rate, then we can have to do with

significant divergences between $(E_p^a - E_{1/2})$ or i_p calculated on the basis of theory and obtained in practice - Fig. 6. From the analytical point of view it is almost of no importance because from the measurements carried out in the same analyzed solution on three different carbon electrodes sufficient resolution of Sb, Bi, Cu, Pb and Tl peaks can be obtained Fig. 10.

However, when electrode processes are investigated on carbon and graphite based Hg films electrodes great divergences of results may take place.

ACKNOWLEDGEMENTS

Support for this study was provided by Interdepartmental Research Program MR-I-32.

REFERENCES

1. Cukrowska E., Cukrowski I., Sykut K.: J. Electroanal. Chem., Part I.
2. Cukrowska E., Cukrowski I., Sykut K.: J. Electroanal. Chem., Part II.
3. Sykut K., Cukrowski I., Cukrowska E.: J. Electroanal. Chem., 115 137 (1980).
4. Cukrowski I.: Patent No 106555 Poland (1978).
5. Matson W. R., Roe K., Carrit D. E.: Anal. Chem., 37 1594 (1965).
6. Hume N., Carter J. N.: Chem. Anal., 17, 747 (1972).
7. Štulikova M.: J. Electroanal. Chem., 48, 33 (1973).
8. Morcos I.: J. Electroanal. Chem., 50, 373 (1974).
9. Morcos I.: J. Electroanal. Chem., 54, 87 (1974).
10. Yaniv D., Ariel M.: J. Electroanal. Chem., 79, 159 (1977).
11. Laser D., Ariel M.: J. Electroanal. Chem., 52, 474 (1974).
12. Cukrowski I., Cukrowska E., Sykut K.: J. Eletroanal. Chem., 125, 53 (1981).
13. Pluta M.: Mikroskopia optyczna, PWN, Warszawa 1982.
14. Clem R. G., Litton G., Ornelas L. D.: Anal. Chem., 45, 1306 (1973).

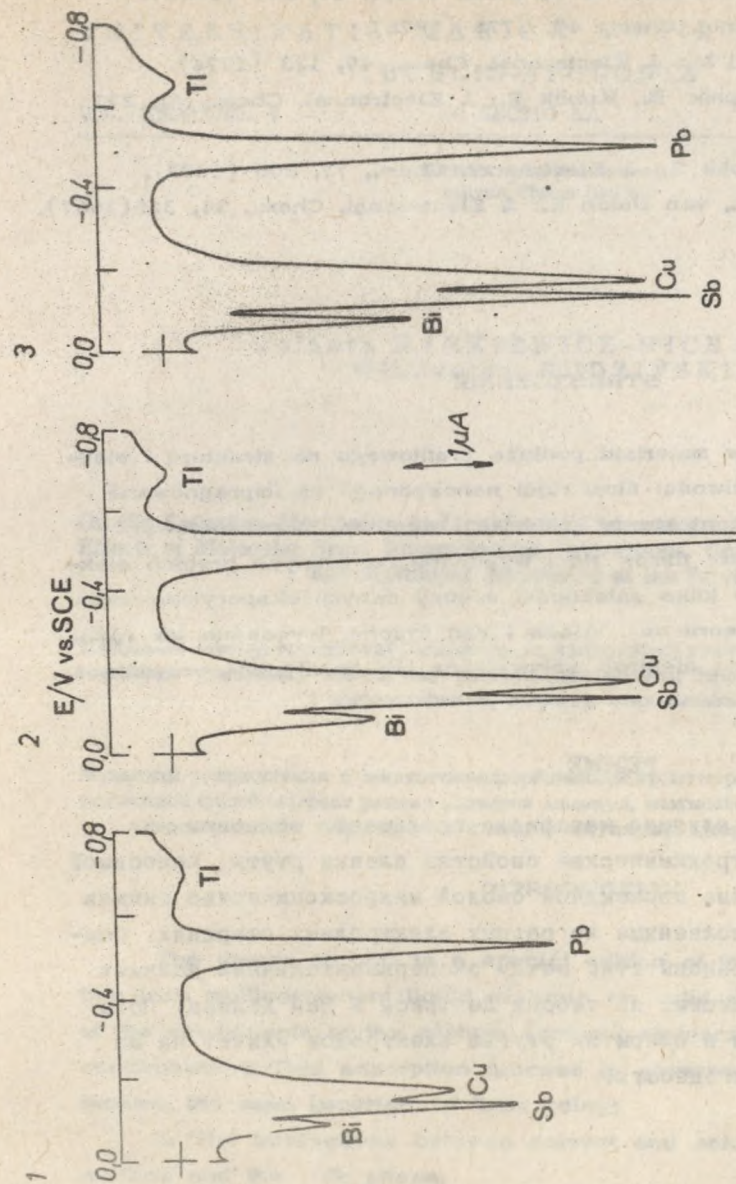

Fig. 10. The dependence of the shape of Bi, Sb, Cu, Pb and Tl ASV curves on the carbon electrode kind: (1) GC, (2) KOM 3, (3) KW II. Solution: 0.1M HCl, $2.5 \cdot 10^{-5}$M Hg^{2+}, $1 \cdot 10^{-7}$M Bi^{3+}, $2 \cdot 10^{-7}$M Sb^{3+}, $3 \cdot 10^{-7}$M Cu^{2+}, $3 \cdot 10^{-7}$M Pb^{2+} and $8 \cdot 10^{-7}$M Tl^{1+}. Deposition potential -1V. Deposition time 2 min. Scan rate 3,083Vs^{-1}

15. Clem R. G., Sciamanna A. F.: Anal. Chem., 47, 276 (1975).
16. Clem R. G.: Anal. Chem., 47, 1778 (1975).
17. Laser D., Ariel M.: J. Electroanal. Chem., 49, 123 (1974).
18. Stojek Z., Stępnik B., Kublik Z.: J. Electroanal. Chem., 74, 277 (1976).
19. Stojek Z., Kublik Z.: J. Electroanal. Chem., 77, 205 (1977).
20. de Vries W. T., van Dalen E.: J. Electroanal. Chem., 14, 315(1967).

STRESZCZENIE

Badano wpływ materiału podłoża grafitowego na strukturę i elektrochemiczne właściwości filmu rtęci nanoszonego na impregnowane żywicą epoksydową elektrody grafitowe i węglowe. Zaprezentowano zdjęcia mikroskopowe filmów rtęci wykonane na różnych prętach elektrodowych. Opisano kilka zależności między danymi eksperymentalnymi a wynikającymi z teorii de Vriesa i Van Dalena. Wykazano jak różnice w pokryciu rtęcią elektrod wpływają na ich analityczną przydatność.

РЕЗЮМЕ

Исследовали влияние материала графитного основания на структуру и электрохимические свойства пленки ртути, наносимой на импрегнированные эпоксидной смолой микроскопические снимки пленок ртути, выполненные на разных электродных стержнях. Описали несколько зависимостей между экспериментальными данными и данными, вытекающими из теории Де Фриса и Ван Далена. Показали, что разницы в покрытии ртутью электродов влияют на их аналитическую пригодность.

Złożono w Redakcji 12.03.1985.